A Biomechanical Assessment of the Structural Response to Dynamic Belt Loading of the Hybrid III 6yo Abdominal Insert

J. F. Lamp, R. W. Kent
The Center for Applied Biomechanics; University of Virginia

The high rate of abdominal injuries, particularly in children, related to loading of the seatbelt in automotive impacts demands that crash dummies exhibit better biofidelity. Motivated by field data, Elhagediab et al, in 2007, constructed a silicone gel-filled abdominal insert for the Hybrid III six-year-old dummy to improve its biofidelity under a variety of loading conditions and sample pertinent data for the assessment of injury risk. These tests aimed to assess the biofidelity of the pediatric abdominal insert by comparing its loading response to that of the porcine pediatric abdomen model developed by Kent et al in 2006. In the same test fixture and under the same loading conditions, in-situ in the Hybrid III dummy, the abdominal insert was belt-loaded across the abdomen at three different velocities, two different belt angles, two different penetration depths, and both with a neoprene jacket and without the jacket. High speed video of each test as well as reaction force, belt force, acceleration at the belt midline and on the tabletop, as well as a dummy outputted chest deflection and lumbar forces were recorded. The data was analyzed and compared to Kent's porcine model in order to assess the biomechanical response of the abdominal insert. The insert was found to match the porcine model kinematics and rate insensitivity, but the overall stiffness was too compliant and the insert lacked the same inertial response at the onset of loading characteristic of the porcine model.

INTRODUCTION

In car accidents involving children the abdomen is the second most commonly injured region of the body (Durbin et al. 2001; Bergqvist et al. 1985; Tso et al. 1993; Trosseille et al, 1997). It is also known that children between 4 and 8 years of age are 24.5 times more likely to sustain a moderate or worse (AIS2+) abdominal injury than younger children, and 2.6 times more likely than older children (Arbogast, 2004). In a case study of 98 children with "seat belt syndrome" defined as any of a set of injuries commonly caused by belt restraint loading, including abdominal injuries and lumbar spinal fractures, the mean age was 7.3 years, and 72% were between 5 and 9 years old.

Based on the field data this age group lacks the specified protection it requires during a car crash. According to the National Highway Traffic Safety Administration (NHTSA) children aged 4 to 8 and less than 4'9" stature should be seated in booster seats, yet Partners for Child Passenger Safety report that the most common form of restraint used for children 5 years and older is the adult seatbelt. When improperly restrained, such as with adult seatbelts, children can sustain abdominal injuries even during low severity impacts (Arbogast, 2007). Arbogast et al. (2007) discussed some of the mechanisms for these injuries in a case study of 21 seatbelt restrained children who, during an accident, suffered moderate or worse internal abdominal injuries. The most common mechanism recorded was direct compression of the injured abdominal organ, and three particular kinematic patterns were identified to elicit such compression. Presubmarining was described as automotive impact with the belt initially positioned too high so that pelvis was not loaded, while classic submarining occurred when a reclined child slid under a properly positioned lap belt, causing loading of the abdomen. Submarining and jackknifing occurred when the pelvis slid under the lap belt while the torso pitched forward as it would if the shoulder belt were not worn. Currently the standard Hybrid III 6-year-old crash test dummy does not reproduce any of these kinematic patterns due to a poorly shaped pelvis and lack of abdominal biofidelity and instrumentation (Arbogast, 2005). To address this need a large collaborative effort was undertaken as described in Arbogast et al. (2005), with the goal of enhancing the shape of the Hybrid III 6-year-old pelvis and developing an abdominal insert mechanically similar in response the a child's abdomen with instrumentation capable of measuring belt penetration into the abdomen. The purpose of the study is to assess the mechanical biofidelity of the abdomen insert proposed and developed by Elhagediab et al. in (2007).

In 2006, Kent et al. published the results of a study that both developed a porcine model for the 6 year-old abdomen and presented the biomechanical response of the model under dynamic belt loading. In 2007, Elhagediab et al. developed a child sized instrumented abdominal insert for the Hybrid III dummy. The present study proposes to characterize the mechanical response of the Hybrid III 6-year-old abdominal insert under belt loading and to compare its response to that of the porcine abdominal model developed by Kent et al (2006). All three studies are parts of a larger collaborative effort to modify the Hybrid III 6-year-old dummy in order to make it capable of accurately assessing injury risk in the crash test environment as described in Arbogast et al. (2005).

The porcine abdominal model described above was developed to represent a 6-year old human by comparing 8 anatomical parameters relating to subject geometry and inertial properties

(Kent et al. 2006). The optimization yielded a 77-day-old pig weighing 21.4 kg as the target model for the abdominal anatomy of a 6-year-old child without any need for scaling. The model was validated against quasi-static, non-injurious child volunteer data published by Chamouard et al. (1996). The abdominal penetration vs. reaction force data obtained from the porcine model, in similar testing conditions to the Chamouard tests, was shown to fit in the Chamouard corridors. This provided a limited but promising validation of the porcine abdominal model under quasi-static belt loading. The porcine model was also loaded in a variety of more severe loading conditions to characterize its response in an environment associated with that of a car crash. Based on the range of dynamic tests conducted, the porcine model of the pediatric abdomen was found to have a negligible effect from muscle stimulation, loading rate insensitivity in the lower abdomen, and little effect from loading location except when tested at the highest loading rate, in which case the upper abdomen response was stiffer. In addition to these findings the study produced a series of reaction force and belt force vs. abdominal penetration plots that are useful for comparison with the Hybrid III 6-year-old abdominal insert developed by Elhagediab et al. (2007).

METHODS

Testing Device

The table top belt loading fixture used during the porcine tests (Figure 1) was reassembled to test the Hybrid III 6-year-old abdominal insert. The fixture is designed for belt loading of a subject positioned supine on the table top at different velocities, penetration depths, belt angles, and waveforms, including ramp-hold (loaded to a specified depth and held) and ramp-release (loaded to a specified depth and then released). A hydraulic hose quick-release link released the loading bar at a specified piston travel depth. The frame of the fixture was anchored to the concrete floor in the testing room for stability and reduction of vibrations. A 500lb single axis load cell was mounted beneath each of the four corners of the table top to measure the vertical reaction load. The table top rested on acorn nuts attached to the load cells to prevent the transmission of shear loads. This configuration would have allowed the table top to slide on the acorn nuts, thus

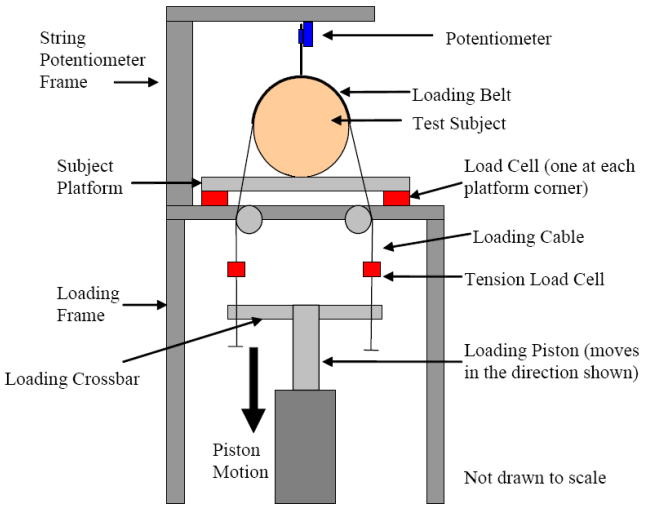

Figure 1: Table top belt loading test fixture

journal bearings were installed to prevent lateral and longitudinal movement of the table with respect to the fixture. A pneumatic piston drove an aluminum crossbar attached to the loading belt through a quick release mechanism. Two tension load cells measured the inline belt force, an accelerometer and photo target were used to measure the mid-line belt motion, and a second accelerometer measures the vibrations of the table.

Test Conditions

The primary objective of this test series was to produce Hybrid III abdominal insert data that is useful for comparison to the porcine pediatric abdomen model developed by Kent et al (2006). With this objective in mind, the controlled conditions for each test were developed to replicate the conditions of the porcine tests whenever feasible. Five different parameters were controlled in the porcine tests including loading location, waveform, muscle tensing, belt displacement, and belt displacement rate. Loading location was not varied during this test series primarily due to the size of the abdominal insert, which would not accommodate two loading positions without directly engaging other aspects of the dummy. Muscle tensing is another test condition that was not reproduced in the abdominal insert test series because the insert is not designed to make that distinction. Three variable test conditions were therefore kept similar to the porcine test as well as an additional test condition, belt wrap angle, which appeared to be of interest in this series. A higher belt wrap angle was expected to cause a stiffer abdominal response in seatbelt loading. Thus two different belt wrap angles were selected; a high belt wrap angle of 175° as well as a lower angle of 150°(see figure 2 for an explanation of belt wrap angle). The four controlled parameters were waveform (ramp-release RR, and ramp-hold RH), belt displacement (shallow: 25mm, and deep: 55mm), belt displacement rate (low: 1.6m/s, mid: 3.8m/s, and high: 6.7m/s), and belt wrap angle (low: 150°, and high: 175°). The Hybrid III 6 year old dummy was shipped with a neoprene, wetsuit-like, jacket that seemed to stiffen the response of the abdomen when installed on the dummy. Nine additional tests were conducted to characterize this difference. The test matrix consisted of fifty-nine tests; however, only 42 were completed due to a rupture in the abdominal insert. Completed tests conditions included all dynamic ramp-release tests with the neoprene jacket as well as without the jacket with the exception of three (Table 1 of the Appendix includes all completed tests).

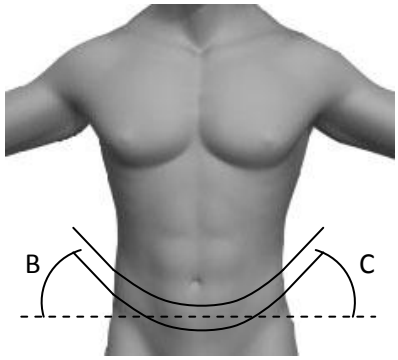

Figure 2: Belt wrap angle is the sum of angles B & C

Test Procedure

For all tests and trials the Hybrid III dummy was placed supine on the loading surface, imitating the matching porcine tests with the belt situated midway between the pelvis and the

ribs on the abdominal insert, exactly 110 mm inferior of the superior edge of rib number 2. The quick release mechanism was configured to disengage the piston at the maximum penetration point, either 55mm or 25mm, or disabled during a ramp-hold test according to the test matrix. All data was exported and saved, and photographs were taken to document post-test conditions.

Analysis

All sensors were recorded at 5 kHz and filtered according to the Society of Automotive Engineers (1988) J211 recommendations. Video was also recorded at 5 kHz and belt displacement was derived from the videos using point tracking software and a known in-plane reference for calibration. The initiation of each test sequence, the video recording, and the sensor data acquisition were controlled by a single trigger. The four vertical reaction load cells were summed to produce the total reaction force on the table top, and the two belt tension load cells were averaged to produce the belt tension. The velocity for each test was determined by calculating the slope of the displacement data between point closest to 40 percent of total displacement and the point closest to 80 percent of total displacement.

RESULTS

Forty-one belt loading tests were conducted before a rupture in the abdominal insert rendered the test series complete without finishing eighteen of the tests. Two other tests were left out of this study due to a malfunction of the data acquisition trigger. As a result only ramp-release dynamic tests, both with and without a jacket, were included, and among those three out of thirty-six are missing from the no-jacket dynamic tests and all nine jacket tests are included. All tests completed are listed in the final test matrix (Table 1 of the Appendix). The time history of belt tension, reaction force, and abdominal penetration from a representative dynamic test (ABINS2.09) is shown in figure 3. Time, on the x-axis, references the trigger event as time zero; this automatically synchronized the camera and data acquisition with the initiation of each test. From this plot it can be shown that belt displacement increases with belt tension. This was common from test to test and likely indicates a low contribution from inertia to the overall mechanical response of the abdomen. This is unlike the porcine model for which the belt force built faster than the displacement during the first few milliseconds of loading. The difference may be the result of the lack of distinct organ masses in the insert which would increase the inertial contribution with the onset of belt motion. The insert seems to rely primarily on stretching of the elastic shell to control the mechanical response. From the same time-history plot the reaction force seems to lag behind the belt force by about 7ms and then peaks at more than 2.5 times that of the belt force. This lag and subsequent high peak reaction force is similar to that of the porcine model and represents the internal response of the subject as energy from the belt is transferred to the dorsal boundary condition.

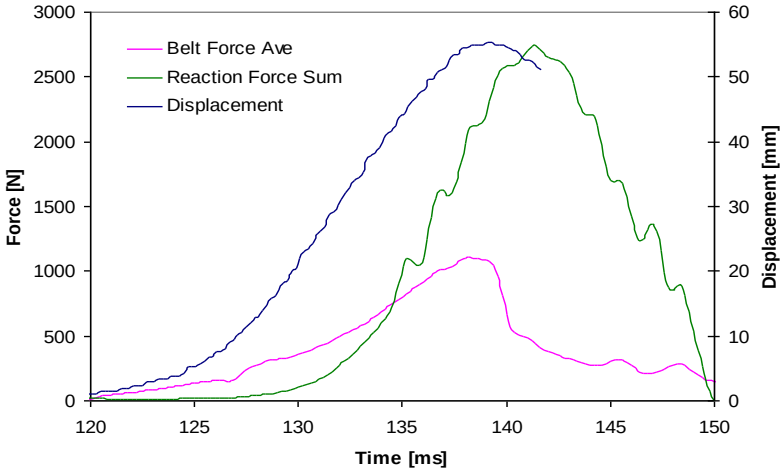

Figure 3: Time history plot of belt tension, reaction force, and belt displacement

All dynamic tests completed without the neoprene jacket are plotted in the belt force vs. abdominal penetration graph in figure 4 along with corridors representative of the corresponding porcine model response data. The bulk of the tests lie just below the porcine model corridors indicating that the dynamic response of the insert is too compliant. The overall stiffness of the insert was about half that of the porcine model.

Figure 5 depicts all of the dynamic tests conducted without the jacket plotted and colored by velocity. The equal spread indicates a lack of rate dependence in the insert, similar to the lower abdomen porcine model, over the dynamic range tested. The mean belt forces at 20mm of belt displacement were 378 N, 324 N, and 407 N for the low, middle, and high velocity tests respectively. Figure 6 depicts all of the dynamic tests conducted without the jacket plotted and colored by belt angle. The equal spread here indicates a lack of belt wrap angle dependence as well. The mean belt forces at 20mm displacement were 358N and 378N for 150 degrees and 175 degrees respectively. Figure 7 compares belt force vs. abdominal deflection data obtained from all the dynamic tests conducted with the jacket to corridors representative of the data collected without the jacket. It was expected that the jacket would slightly, perhaps not noticeably, stiffen the insert response. This was not exactly the case though. The jacket seemed to consistently change the shape of the curve, although only three of the jacket tests were outside of the range of the no-jacket responses. These three, however, were all conducted at the highest velocity of approximately 6.7m/s. This indicates that the jacket may introduce rate dependence; however, too few tests were done to establish any conclusive results about the complicated interaction observed between the insert and the jacket.

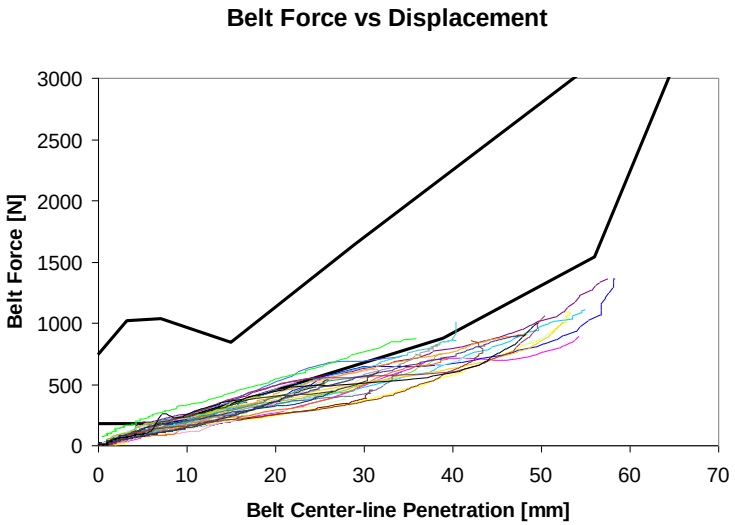

Figure 4: Belt force vs. displacement for dynamic tests plotted with porcine model corridors in black

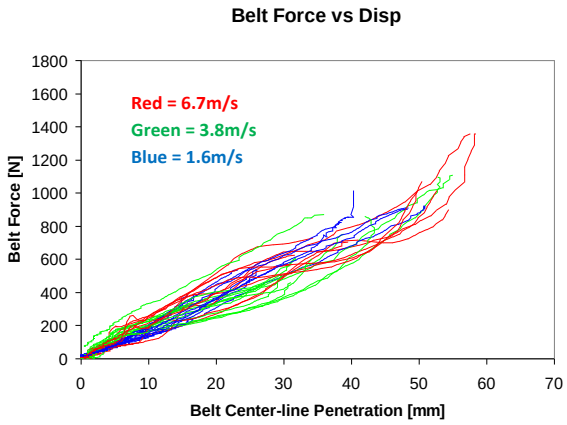

Figure 5: Belt force vs. displacement colored by velocity

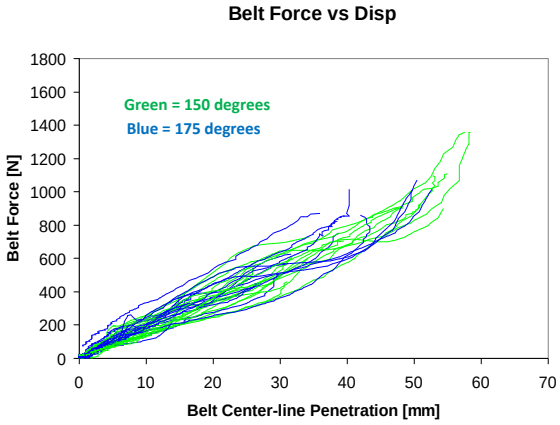

Figure 6: Belt force vs. displacement colored by belt wrap angle

DISCUSSION

This series of tests has contributed data to characterize the abdominal insert developed by Elhagediab et al. (2007) and compared the data with that of the porcine model developed by Kent et al. (2006). Because the elastic shell thickness of the insert can be adjusted to tailor its response, the overall stiffness of the abdomen was considered secondary in importance to the insert's kinematic response and sensitivity to crash environmental factors such as rate and belt angle.

Video analysis revealed several similarities in the kinematic response of the abdominal insert to that of the porcine model. Figure 8 shows the belt loaded abdomens of both the Hybrid III six-year-old dummy with the insert and jacket installed and the porcine model side-by-side. Notice the ventral bulge in the pelvis inferior to the belt in both pictures. As the belt loaded the porcine model, soft organs such as the small intestines escaped longitudinally creating a bulge in the pelvis and presumably displacing the diaphragm in the superior direction. The insert responded similarly with liquid gel in place of the organs. Figure 9 shows the kinematics in the superior direction of the insert more clearly. As the belt displaces the liquid gel the superior aspect of the abdomen expands into the thoracic cavity of the dummy as it does in humans (Coermann, 1960; Lamielle, 2008). Another kinematic response observed in figure 8 is the engagement of the ribcage.

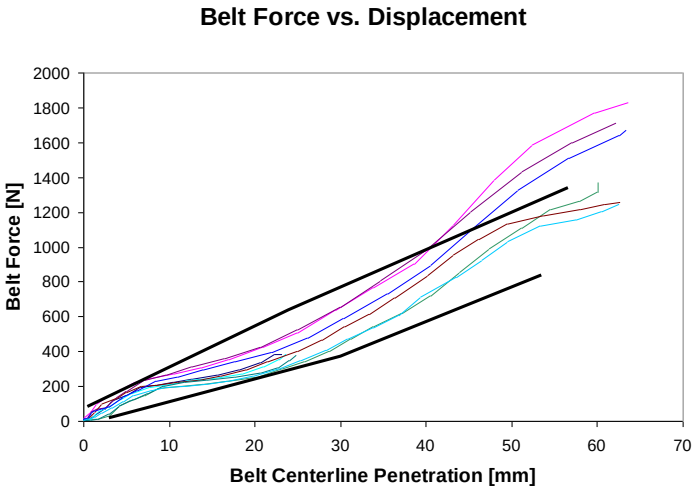

Figure 7: Belt force vs. displacement plot of jacket test and corridors for no-jacket tests in black

Although the distance between the pelvic region and the ribcage in the porcine model is greater than that of a six-year-old child, it appears that the neoprene jacket plays an analogous role of engaging the dummy ribcage as the skin of the porcine model. Such interactions between different biological components are difficult to reproduce in a dummy, but are very important in achieving an acceptable holistic dummy response in a crash environment.

Figure 8: Video capture from tests (H3 6yo left, porcine model right)

As mentioned earlier the insert ruptured during one of the final dynamic ramp-release tests. At this time the insert had been loaded a total of 72 times including the 30 trials runs not included in the results of this series. The rupture occurred at one of the bolts that passed through the metal dummy interface on the outside of the shell through the shell wall and into a plastic plate on the inside of the shell. Even though the metal interface and plastic plate clamp the shell wall, one of the bolt holes stretched enough to allow some of the liquid gel to pass through it.

CONCLUSIONS

This study characterized the structural response of the insert under belt loading and compared its response to that of the porcine model developed by Kent et al. (2006). From the time-history plots the inertial response of the insert was found to be lacking compared to the porcine model in the onset of loading. This issue may be insurmountable due to the impracticality of modeling individual organ masses in a dummy. Belt force and displacement data was used to assess the overall stiffness as well as angle and belt rate sensitivity. It was concluded that the insert was more compliant than the porcine model, but matched the rate insensitivity of the

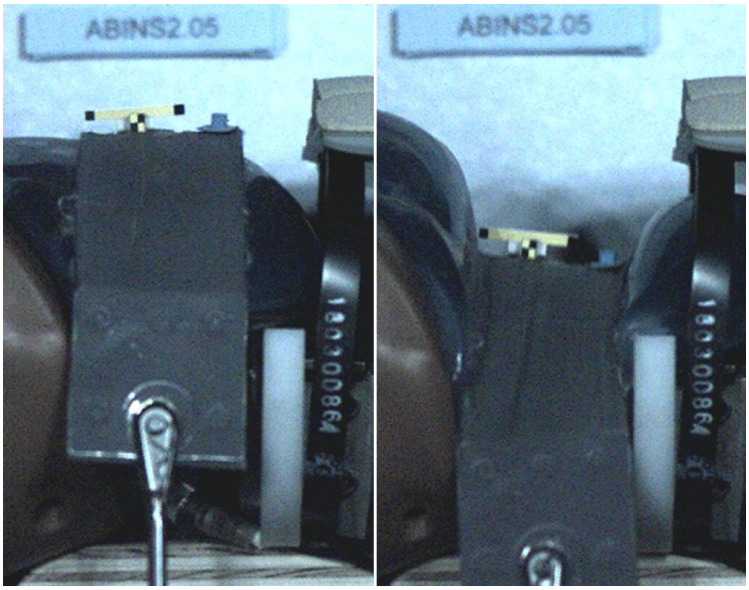

Figure 9: Video capture from test; before and during belt loading

porcine model, and likewise showed no belt wrap angle sensitivity. The kinematics of the insert were assessed from the video and found to be similar to those of the porcine model and the human abdominal cavity under belt loading.

ACKNOWLEDGEMENTS

We acknowledge Steven Rouhana at Ford for sending the abdominal insert to the Center for Applied Biomechanics for testing as well as advice. We acknowledge VRTC for allowing the Center for Applied Biomechanics to borrow a Hybrid III 6-year-old dummy for this project. Autoliv is also acknowledged for providing the funds necessary for the completion of this test series.

REFERENCES

ARBOGAST, KB; MONG, A; MARIGOWDA, S; KENT, RW; STACEY, S; MATTICE, JM; TANJI, H; HIGUCHI, K; ROUHANA, SW (2005) Evaluating Pediatric Abdominal Injuries. Paper 05-0046, Proceedings of the 19th International Technical Conference on the Enhanced Safety of Vehicles (ESV).

ARBOGAST, KB; KENT, RW; MENON, RA; GHATI, Y; DURBIN, DR; ROUHANA, SW (2007) Mechanisms of Abdominal Organ Injury in Seat Belt-Restrained Children. Journal of Trauma, 62(6): 1473-1480.

CAVANAUGH, JM; NYQUIST, GW; GOLDBERG, SJ; KING, AI; (1986) Lower Abdominal Impact Tolerance and Response. Stapp Car Crash Conference Proceedings, Paper 861878.

COERMANN, RR;ZIEGENRUECKER, GH;WITTWER, AL;VON GIERKE, HE; (1960) The Passive Dynamic Mechanical Properties of the Human Thorax-Abdomen System and of the Whole Body System. Aerospace Medicine, 31: 443-455.

ELHAGEDIAB, A; HARDY, W; ROUHANA, SW; KENT, RW; ARBOGAST, K; HIGUCHI, K (2007) Development of an instrumented rate-sensitive abdomen for the six year old Hybrid III dummy. JSAE Annual Congress, Yokohama, Japan.

KENT, RW; CRANDALL, JR; RUDD, RW; LESSLEY, DJ (2002) Load Distribution-Specific Viscoelastic Characterization of the Hybrid III Chest. Paper 2002-01-0024, Society of Automotive Engineers.

KENT, RW; STACEY, S; MATTICE, JM; KINDIG, M; FORMAN, J; WOODS, WA; EVANS, J (2006) Assessment of abdominal injury criteria for use with pediatric seatbelt loading. Proceedings of the 5th World Congress of Biomechanics, Munich, Germany, abstract in J. Biomech. 39(1):S159.

LAMIELLE, S; VEZIN, P; VERRIEST, JP; PETIT, P; TROSSEILLE, X; VALLANCIEN, G. (2008) 3D Deformation and Dynamics of the Human Cadaver Abdomen Under Seatbelt Loading. Stapp Car Crash Journal, 52: 267-294.

MILLER, MA (1989) The Biomechanical Response of the Lower Abdomen to Belt Restraint Loading. Journal of Trauma, 29(11): 1571-1584.

NUSHOLTZ, G; KAIKER, P (1994) Abdominal Response to Steering Wheel Load. International Technical Conference on the Enhanced Safety of Vehicles (ESV), 14.

ROUHANA, SW (1989) Assessing Submarining and Abdominal Injury Risk in the Hybrid III Family of Dummies. Stapp Car Crash Conference Proceedings, Paper 892440.

ROUHANA, SW; ELHAGEDIAB, AM; WALBRIDGE, A; HARDY, WN; SCHNEIDER, LW (2001) Development of a Reusable, Rate-Sensitive Abdomen for the Hybrid III Family of Dummies. Stapp Car Crash Journal, 45: 33-60.

APPENDIX

Table 1: Final Test Matrix

Test Matrix

Test	Velocity [m/s]	Belt Wrap Angle	Penetration [mm]	Waveform	Jacket [on/off]
ABINS1.01	1.6	175	25	RR	on
ABINS1.02	6.7	150	55	RR	on
ABINS1.03	3.8	150	55	RR	on
ABINS1.04	1.6	175	25	RR	on
ABINS1.05	6.7	150	55	RR	on
ABINS1.06	3.8	150	55	RR	on
ABINS1.07	1.6	175	25	RR	on
ABINS1.08	6.7	150	55	RR	on
ABINS1.09	3.8	150	55	RR	on
ABINS2.01	1.6	175	25	RR	off
ABINS2.02	6.7	150	55	RR	off
ABINS2.03	3.8	150	55	RR	off
ABINS2.04	1.6	175	25	RR	off
ABINS2.05	6.7	150	55	RR	off
ABINS2.06	3.8	150	55	RR	off
ABINS2.07	1.6	175	25	RR	off
ABINS2.08	6.7	150	55	RR	off
ABINS2.09	3.8	150	55	RR	off
ABINS2.10	1.6	150	55	RR	off
ABINS2.12	3.8	175	25	RR	off
ABINS2.13	1.6	150	25	RR	off
ABINS2.14	3.8	175	25	RR	off
ABINS2.15	6.7	175	25	RR	off
ABINS2.16	1.6	150	25	RR	off
ABINS2.17	3.8	150	25	RR	off
ABINS2.18	6.7	150	25	RR	off
ABINS2.19	1.6	175	55	RR	off
ABINS2.20	3.8	175	55	RR	off
ABINS2.21	6.7	175	55	RR	off
ABINS2.22	1.6	150	55	RR	off
ABINS2.23	6.7	150	25	RR	off
ABINS2.24	3.8	150	25	RR	off
ABINS2.25	1.6	175	55	RR	off
ABINS2.26	3.8	175	25	RR	off
ABINS2.27	6.7	175	25	RR	off
ABINS2.28	1.6	150	25	RR	off
ABINS2.29	3.8	150	25	RR	off
ABINS2.32	3.8	175	55	RR	off
ABINS2.33	6.7	175	55	RR	off
ABINS2.34	1.6	150	55	RR	off
ABINS2.35	6.7	175	55	RR	off
ABINS2.36	3.8	175	55	RR	off